A Model of the Human Visual System in Its Response to Certain Classes of Moving Stimuli

David H. Foster
Imperial College of Science and Technology, Applied Optics Section,
Department of Physics, Prince Consort Road, London S.W. 7

Received August 22, 1970

Abstract. The purpose of this study is to construct a functional model of the human visual system in its response to certain classes of moving stimuli.

Experimental data are presented describing the interdependence of the input variables, temporal frequency, spatial period, etc., for two constant response states, viz. threshold motion response and threshold flicker response. On the basis of these data, two basic units are isolated, a vertical (V) unit and a horizontal (H) unit. The H-unit is identified with the Reichardt multiplier (Reichardt and Varju, 1959), and the V-unit with the de Lange filter (de Lange, 1954).

A definition of the general motion response of the H-units is obtained, and this is then reduced to an expression which may be applied directly to the observed motion response data. By this method, Thorson's simplification of the Reichardt scheme (Thorson, 1966) is adopted for the H-unit and total and relative (population) weighting factors, associated with the H-unit output, are defined.

In order to reconcile the theoretical square-wave threshold motion response with the experimental data, Thorson's simplification is modified with the introduction of a low-pass filter on the output. The amended scheme is shown to predict a (temporal) frequency-dependent phase-sensitivity. This prediction is tested experimentally, and its validity indicated.

1. Introduction

This work is concerned with the construction of a functional model of the human visual system in its response to certain classes of moving stimuli. The analysis is based partly on two earlier studies (Foster, 1969, 1970b), and the intention here is to present a unified treatment of the observed data, with special emphasis on the description of the system model.

The first step in this examination of the visual system is to establish a more precise definition of the system, in terms of input and output variables, and to determine an appropriate method of analysis.

1.1. Output Specification and General Method of Analysis

In this section we define the output of the system and describe the general method of analysis to be employed.

It has been shown (Foster, 1968) that in the visual perception of certain configurations of moving spatially-periodic stimuli, there exist transitions in sensation associated with certain critical values of the temporal frequency, f. Thus, as f is increased from small values, we have the following:

i) For $f \leqq f_l$ (f_l, the lower critical frequency): a sensation of well-defined directed motion, (providing f is not too small).

ii) For $f_l < f \leqq f_u$ (f_u, the upper critical frequency): a sensation of motion without well-defined direction, or non-uniform flicker.

iii) For $f > f_u$: fusion.

Therefore, we may distinguish two component variables in the system output: one giving information about the local temporal fluctuations of the stimulus (variable $O1$, say), and the other giving information about the spatial ordering of these local temporal fluctuations (variable $O2$, say). For $f \leqq f_l$, both $O1$ and $O2$ contribute to the total response; for $f_l < f \leqq f_u$, only $O1$ contributes; for $f > f_u$, neither $O1$ nor $O2$ contributes.

The direct measurement of output variables, $O1$ and $O2$, as functions of some chosen input variable, is not a practicable method of analysis in the present case, since the output is inaccessible. An alternative approach is the following.

We set the chosen output variable equal to some arbitrary constant value, and then determine the interdependence of the chosen input variables such that the condition of output constancy is maintained. In the present case, the just detectability of the time-varying nature of the stimulus ($f = f_u$) may be associated with the magnitude of output variable $O1$ just exceeding some fixed threshold level; similarly, the just detectability of a well-defined stimulus direction ($f = f_l$) may be associated with the magnitude of the output variable $O2$ just exceeding some other fixed threshold level. By working at one of these two threshold output states, we thus hold constant either $O1$ or $O2$. This is the method of approach adopted here.

1.2. Input Specification and General Stimulus Configuration

To complete the specification of the system (in terms of input-output variables), it is necessary to define the form of the input array and to define the range of the stimulus variables. This we now do.

Two properties that the system should demonstrate are the following:

i) A fixed input (receptor) array.

ii) A uniform density of associated processing units.

In order to approximate these characteristics, we adopted the experimental arrangement described below.

The primary stimulus was provided by a rotating radial grating. The field of view of this grating was restricted to a foveal annulus. Fixation was assumed to be sufficiently good to maintain (i) above, providing stimulus sensation progressed smoothly to steady-state. Sharp departures from steady-state sensation could be correlated with the presence of flicks (see Ditchburn and Ginsborg, 1953) using other psychophysical cues (see Foster, 1969). [Eye-tremor (Ditchburn and Ginsborg, 1953) was thought not to be a significant factor, in view of the findings of West (1968) and Gilbert and Fender (1969).] The uniformity of response around the annular field, implying (ii) above, was determined by a separate experiment (Foster, 1970a).

With the stimulus configuration described above, the input variables considered were the following: the temporal frequency of the rotating grating, the area of the sectored annulus, the spatial period of the grating, and the waveform of the grating. The modulation depth of the primary stimulus was also included as a variable in one experiment.

The mathematical method chosen for the representation of the system is that of the Laplace transform approach. It was therefore necessary to establish the linearity and the time-invariance of the system. The linearity of the system was prescribed by restricting the input stimuli to small excursions about the mean (background) level (see App. A). The time-invariance of the system, equivalent to the constancy of the subject's observations over some period of time, is discussed in Sec. 3.

Measurements were taken only when the stimulus sensation reached steady-state.

1.3. General Objectives

In the previous two sections, we specified the system in terms of its input and output variables, and outlined the method of analysis to be employed.

In the following sections, the experimental method is described in greater detail, and data are presented for each of the two constant output states. These results are subjected to systematic analysis, and a model of the system constructed.

Two of the principal elements of this model are shown to be a version of the Reichardt multiplier (Reichardt and Varju, 1959) and the de Lange filter (de Lange, 1954). (The latter is a low pass filter which describes, for spatially uniform stimuli, the attenuation characteristics of the human visual system at flicker threshold.)

It will be demonstrated that one of the operations performed by the model is running aurocorrelation (q. v. Licklider, 1951). It will also be shown that the model makes certain predictions concerning the phase sensitivity of the visual system as a function of stimulus frequency. These predictions are tested and their validity indicated.

2. Experimental Apparatus and General Methods

The experimental apparatus used in the present study has been described in detail elsewhere (Foster, 1970a, b); the elements of the system are outlined below.

Referring to Fig. 1, the rotating radial grating, *R.G.*, was transilluminated by the incandescent lamp, L_1, via the liquid filter, F, and diffusing screen, D_1. The view of the grating was restricted with the mask, M, to an annulus of 1.5° total mean angular subtense, and width, 0.21°. Portions of the annulus could be sectioned off; the remaining section was specified by the coordinate, θ (see inset of Fig. 1).

A uniform square background field of total angular subtense, 4.7°, was provided by the light box, L_2, and diffusing screen, D_2.

The primary stimulus field and background field were combined with the beam splitter, P, and the demagnified whole viewed via a 2 mm artificial pupil, *A.P.* Retinal illumination was approximately 390 trolands, and the colour temperature of the background filed, approximately 2500° K.

Both square and sinewave radial gratings were employed: square wave gratings with spatial periods of 40°, 60°, 90°, 120°, 180°, and 360°, and sinewave gratings with spatial periods of 180° and 360°. Deviations of each grating waveform from the ideal were determined to be within the tolerances of the experimental method (Foster, 1970a). The gratings were driven by electric motor, the speed of which was monitered continuously using an electronic tachometer.

A dental bite was used to locate the head of the subject, who fixated, monocularly, the centre of the annular stimulus. The speed of rotation of the radial grating could be controlled by the observer.

Before commencing observations, the primary stimulus was matched by the observer against the background field. A ten per cent neutral density filter was then introduced

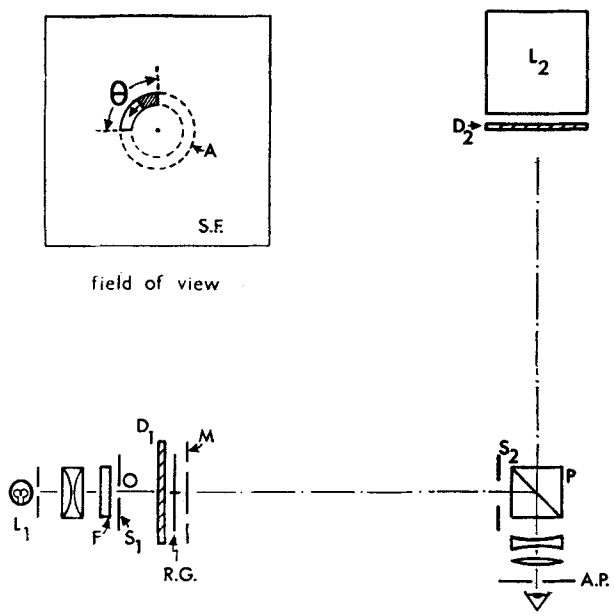

Fig. 1. The experimental apparatus: L_1 and L_2 are incandescent light sources; F, a liquid filter for colour correction; S_1 and S_2, stops; D_1 and D_2, diffusing screens; *R.G.* radial grating; M, annular mask; P, beamsplitter; *A.P.*, artificial pupil
Inset: A, annular aperture; *S.F.*, surround field

between the grating and beam splitter. Thus the stimulus intensity variation was within ten per cent of the background (mean) intensity, and superimposed upon it.

Observers employed were the author who wore correcting contact lenses and was aged 24, G.F. who was aged 20 and was slightly myopic (a correcting lens was introduced), R.A.E. who was emmetropic and aged 22, and W.H.K. who was also emmetropic and aged 42.

3. Experiments and Results

In the following sections results are presented showing the dependence of the temporal frequency, f, upon angular area, θ, and spatial period, λ, at both motion threshold ($f = f_l$) and flicker threshold ($f = f_u$). Data for both sine and square wave stimuli are given. In addition, the de Lange attenuation characteristics, as a function of θ, are described for the present stimulus configuration.

Some preliminary experiments were also carried out in order to establish the uniformity in response around the annular field and the symmetry of the response with respect to reversal of pattern direction. These, and other data showing the stability of response form over periods of several months, are reported in full elsewhere (Foster, 1970a). For the purposes of this present study, data for only two observers are presented for each experiment.

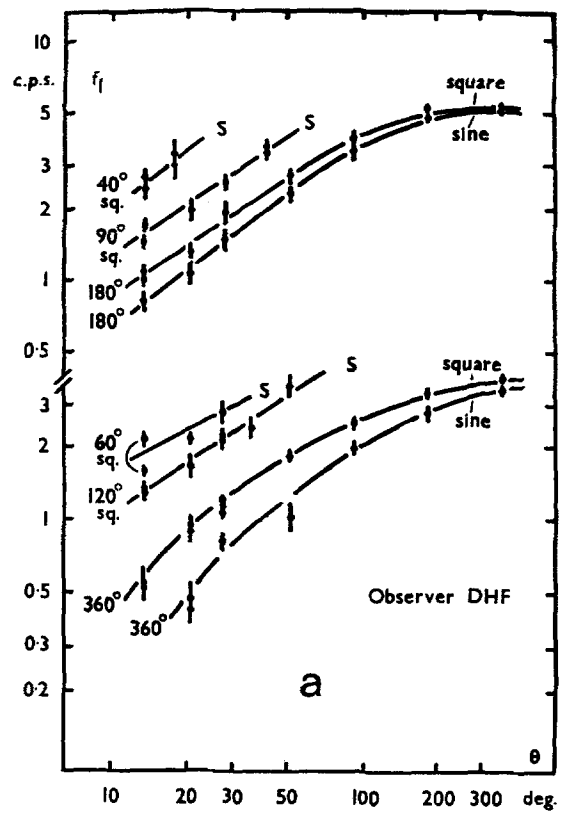

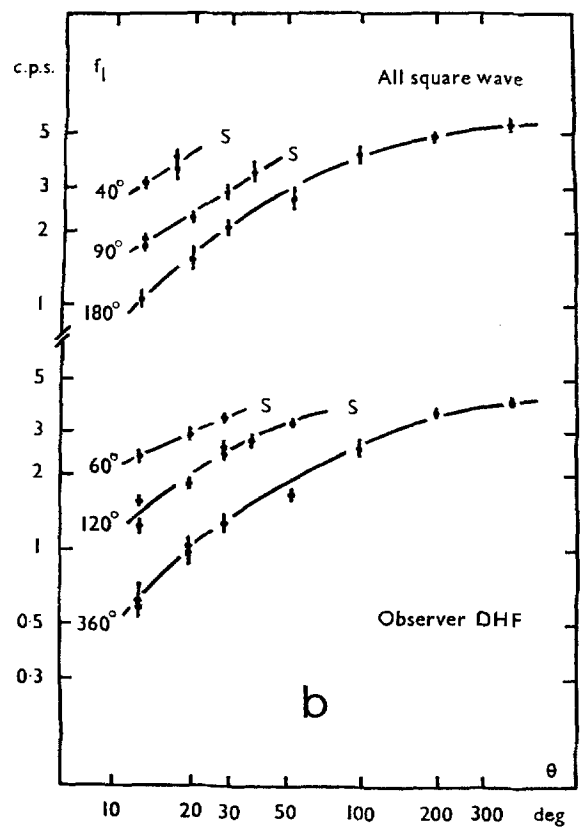

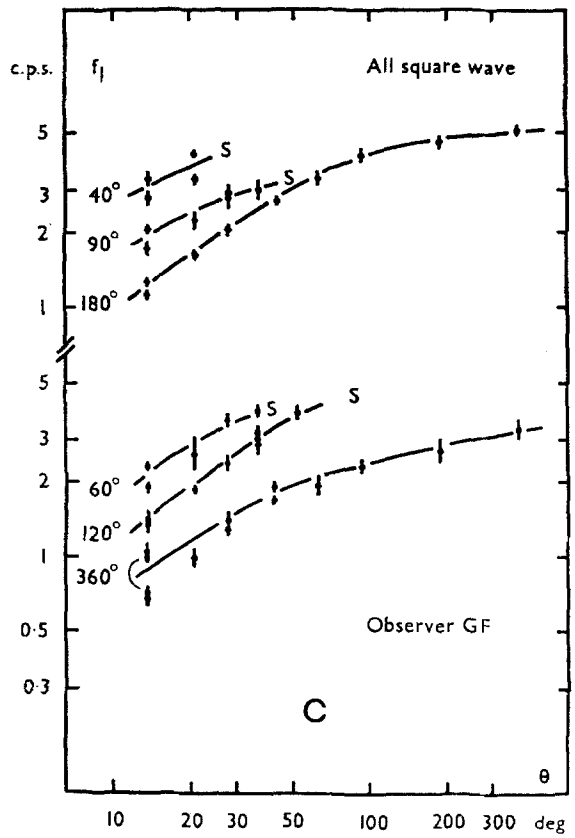

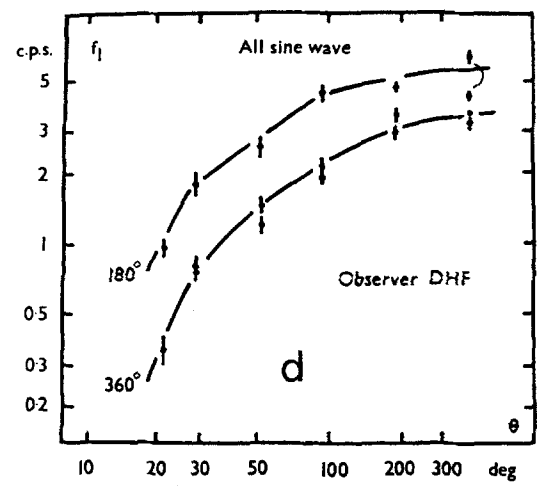

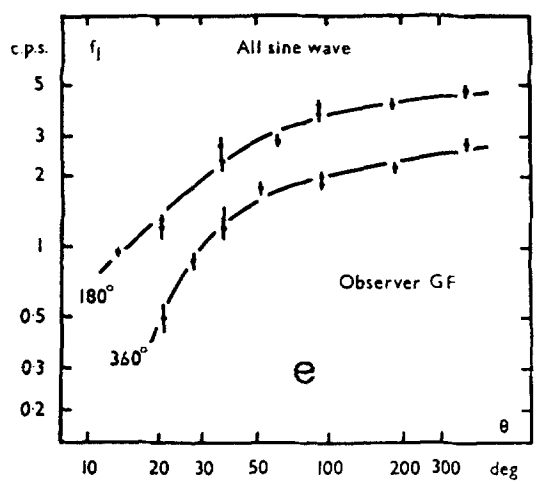

Fig. 2a–e. The dependence of the lower critical frequency, f_l, upon angular area, θ, and spatial period, λ. (The value of λ is shown to the left of each curve.) Results for both sine and square wave gratings are displayed; the onset of the stationary stroboscopic effect is indicated at the points marked "s". The r.m.s. deviation associated with each point is also shown

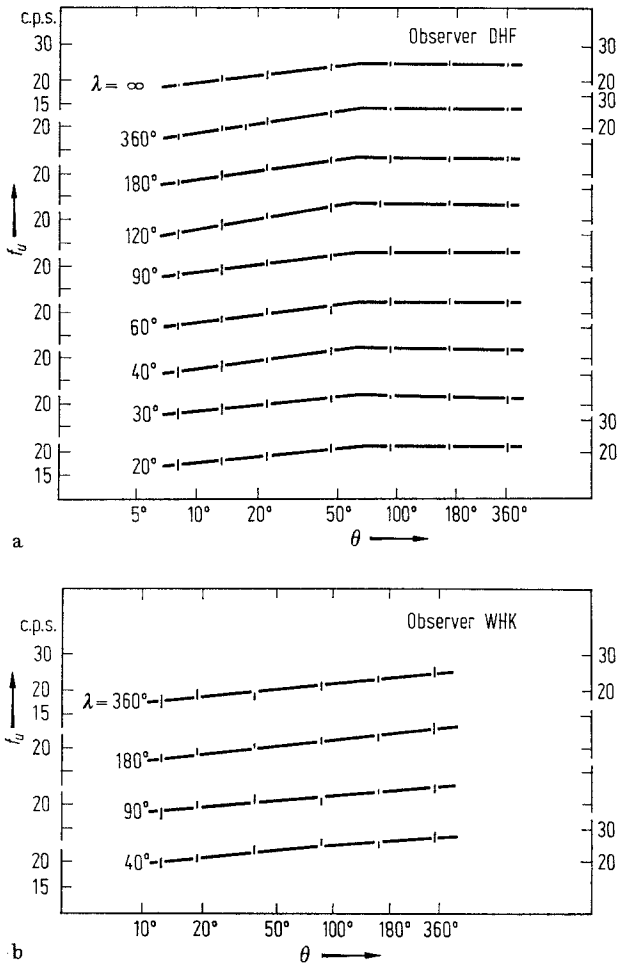

Fig. 3a and b. The dependence of the upper critical frequency, f_u, upon angular area, θ, and spatial period, λ. All waveforms are square and the r.m.s. deviation associated with each point is indicated

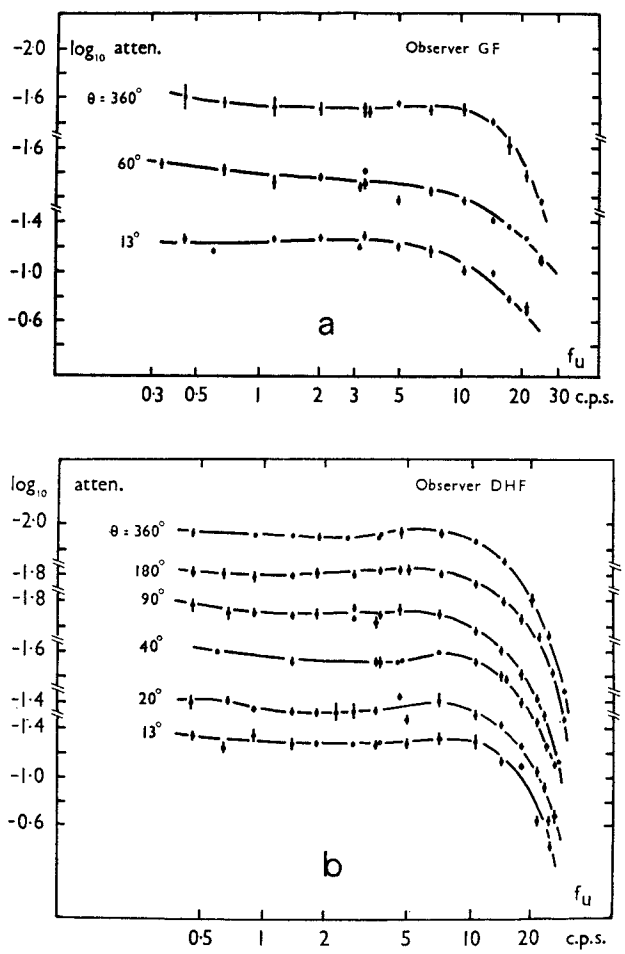

Fig. 4a and b. The de Lange attenuation characteristics at various angular areas, θ. The r.m.s. deviation associated with each point is indicated

3.1. The Dependence of the Lower Critical Frequency, f_l, Upon Angular Area and Spatial Period

The lower critical frequency, f_l, was determined as a function of angular area, θ, for grating periods, λ, ranging from 40° to 360° for square wave stimuli, and 180° and 360° for sinewave stimuli.

The recorded data of Fig. 2 show the general upward trend of f_l with increasing θ and decreasing λ. The sine response curves are depressed with respect to those for square wave stimuli, the difference being most marked at low f_l values.

At certain values of θ and λ, a sensation of well-defined directed motion is not obtainable within the usual range of f_l. This phenomenon is referred to as the "stationary stroboscopic effect" (Foster, 1969). The onset of the effect is indicated in Fig. 2 by the letter "s", and is seen to occur at values of θ just greater than $\lambda/2$, providing $\lambda \leqq 120°$.

3.2. The Dependence of the Upper Critical Frequency, f_u, on Angular Area and Spatial Period

The upper critical frequency, f_u, was also determined as a function of angular area, θ, for a range of grating periods, λ. Square waveform gratings, only, were employed.

The results obtained are displayed in Fig. 3. For each λ value, the curves have been displaced for ease of examination. Included as a limiting case (Fig. 3a) is that of $f_u v.\ \theta$ for infinite spatial period (the latter, a spatially uniform field with temporal modulation, only).

It is seen that the $f_u v.\ \theta$ response is insensitive (within experimental error) to variations in the spatial period, λ.

3.3. The de Lange Attenuation Characteristics as a Function of Angular Area

In order to obtain the de Lange attenuation characteristics for the present experimental configuration, the following modifications were made to the apparatus of Fig. 1.

A rotating sinusoidal grating of 360° spatial period was arranged to interrupt the primary stimulus at its intermediate focus, 0 (thus producing a spatially uniform field with temporal modulation only). A neutral, variable density wedge was also introduced into the system near the stop, S_2.

For a given temporal frequency, f, the subject was required to adjust the modulation depth so that flicker was just descernable. (This is equivalent to

determining the stimulus modulation depth as a function of f_u for infinite λ.)

Note. The visual system has been shown to be linear at flicker threshold (de Lange, 1954; Veringa, 1958) and theoretically there need be no restriction on modulation depths. However, the primary stimulus is superimposed on the background field (see Sec. 2), and variations in modulation depth of the primary stimulus therefore give rise to variations in the total mean level (primary + background). In order to minimise these departures from fixed level working conditions the modulation depth of the primary stimulus is again restricted to ten per cent (see Foster, 1970a).

Attenuation characteristics were thus obtained as a function of the angular area, θ. With the imposed restriction on available modulation depths (see above) the low frequency response, only, could be determined.

In Fig. 4 are shown the low frequency de Lange attenuation characteristics for values of θ ranging from 13° to 360°. The curves have been displaced for ease of examination.

It will be seen that there is no well-defined change in response shape with area, apart from a bodily downward shift with decreasing θ. The overall response is fairly flat, with little differentiation at low frequencies, and breaks to commence the characteristic integration of the de Lange filter (q. v. de Lange, 1954) at approximately 9.0 c.p.s.

4. General Analysis

In the following section, we determine the nature and organization of the constituent elements of the system model. The de Lange filter and the Reichardt multiplier are introduced, and some possible modes of output interaction are examined.

In order to achieve the simplest possible representation of the system, we first make the following assumptions:

i) The system has a well-defined input array (see Sec. 1.2. and Foster, 1970a).

ii) The response of the system is dominated by those units with receptor element pairs lying along the direction of pattern motion (see footnote, Sec. 5.3c).

iii) The population density of functional units is constant around the annular field, and the distribution of units maximally sensitive to clockwise motion is the same as that of units maximally sensitive to anticlockwise motion. (See Sec. 3, and for experimental evidence, Foster, 1970a.)

iv) The contribution of edge effects to the total response is not of primary significance. This is supported by the following:

a) Such effects fail to explain the onset of the stationary stroboscopic effect at angular areas $\theta > 60°$.

b) Such effects are inconsistent with the observed smooth transition of f_1 from $\theta = 360°$ (with no edges perpendicular to pattern direction) to $\theta = 180°$ (with two terminating edges perpendicular to pattern direction). (See Fig. 2.)

We now begin the analysis proper.

4.1. The Nature and Organization of the System's Functional Units

In Sec. 1.1. we distinguished two components to the total system response, viz. $O1$ giving information about the local temporal fluctuations of the stimulus and $O2$ giving information about the spatial ordering of these local temporal fluctuations. Let those sections of the system associated with output $O1$ be termed V-units, and those sections associated with output $O2$ be termed H-units. We now deduce something about the nature and organization of these V- and H-units.

Referring to Fig. 3 it is seen that within experimental error the $f_u v.\ \theta$ response is independent of the spatial period λ. It therefore follows that any interaction between V-units is spatially phase insensitive. [This spatial phase insensitivity is distinct from Reichardt's pattern phase insensitivity and from the single channel phase insensitivity of the visual system discovered by Forsyth (1960).] If we neglect this phase independent interaction, we may represent the V-units by essentially straight-through (vertical) structures.

Referring to Fig. 2 it is seen that the $f_l v.\ \theta$ response *is* a function of spatial period λ, with the stationary stroboscope effect commencing at values of θ up to 60°. It therefore follows that in contrast to the V-units, the H-units involve extensive lateral interaction and may be represented by essentially horizontal formations.

Two possible schemes for the organization of the H- and V-units are shown in Fig. 5. The R represent

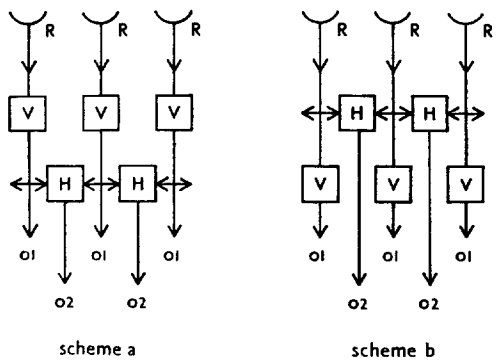

Fig. 5. Two possible schemes for the organization of the H- and V-units. The R represent receptors (or groups of receptors); the channels marked $O1$ carry information about the local temporal fluctuations of the stimulus, and the channels marked $O2$ carry information about the spatial ordering of these local temporal fluctuations

receptors (or groups of receptors) each pair separated by the angular distance, $\Delta\theta$. The two types of output channel $O1$ and $O2$ are indicated.

With scheme (b), the possibility exists that a directed motion response could be observed at some $f_l > f_u$. In practice this is not observed and for the present we adopt scheme (a) to represent the system.

4.2. The Identity of the V- and the H-Units

In this section we show that the V-unit may be identified with the de Lange filter, and the H-unit with some form of Reichardt multiplier.

The V-unit is examined first.

It has been noted (Sec. 3.2) that the variation of the upper critical frequency f_u, with angular area, θ, is independent of the spatial period, λ. This includes the limiting case of $\lambda = \infty$, i.e. a spatially uniform

field. Now the de Lange attenuation characteristics are normally defined for spatially uniform fields, and thus as the most economical assumption, we identify the V-unit with the de Lange filter. The attenuation characteristics of the V-unit, as a function of θ, are therefore given by Fig. 4.

It will be observed in Fig. 4 that the de Lange attenuation characteristics do not exhibit a well-defined change in shape with area, θ, although there is a downward displacement of the curves with reduction in θ. If the sensitivity of the system to variations in θ is attributed solely to threshold variations, which simply shift the basic response along the attenuation axis, θ may then be eliminated from the V-unit description. In this case, the V-units are truly "vertical" (q. v. Sec. 4.1). We shall continue this discussion of the V-unit function in Sec. 5.1.

We now examine the H-unit.

a) Phase Comparison. The fundamental operation performed by the H-unit is that of phase comparison. For completeness we demonstrate that the Reichardt multiplier exhibits such a property.

The response of the Reichardt multiplier to sinewave inputs may be written generally, (q. v. Reichardt and Varju, 1959, and Thorson, 1966) thus:

$$r = G(\omega) \cdot \sin(2\pi \cdot \Delta\theta/\lambda) \qquad (1)$$

where $\omega = 2\pi f$ (f is the temporal frequency), $G(\omega)$ depends on the input waveform and the construction of the multiplier, $\Delta\theta$ is the input pair separation, and λ is the spatial period.

For the H-unit, the phase difference between receptor elements, $2\pi\Delta\phi$ say, may be expressed thus:

$$\begin{aligned} 2\pi \cdot \Delta\phi &= 2\pi \cdot \Delta t/T \\ &= 2\pi \cdot f\Delta\theta/\dot{\theta} \\ &= 2\pi \cdot \Delta\theta/\lambda, \end{aligned}$$

where Δt is the time lag, T is the temporal period of the signal, and $\dot{\theta}$ is the angular velocity of the pattern.

Therefore, Eq. (1) may be rewritten:

$$r = G(\omega) \cdot \sin(2\pi \cdot \Delta\phi). \qquad (2)$$

Thus, the response, r, of the Reichardt multiplier gives a measure of the phase difference between the two time-varying signals incident at each receptor.

b) The Stationary Stroboscopic Effect. We now show identification of the Reichardt multiplier with the H-unit gives rise to an explanation of the stationary stroboscopic effect.

From the curves of Fig. 2 giving $f_l v.\ \theta$ for various λ, it is observed that the stationary stroboscopic effect is only elicited at $\theta > \lambda/2$ (for $\lambda \leqq 120°$). It is also noted [see Eq. (1)] that the Reichardt multiplicative interaction scheme gives positive response values for input pair separations $\Delta\theta < \lambda/2$ and negative response values for $\Delta\theta > \lambda/2$ (providing $\Delta\theta < \lambda$). If the H-unit is identified with the Reichardt multiplier, the stationary stroboscopic effect may be explained in the following way.

For angular areas $\theta < \lambda/2$, the maximum available H-unit input pair separation is less than $\lambda/2$ (since $\Delta\theta \leqq \theta$). According to the Reichardt system, all H-unit outputs are then positive. For $\theta > \lambda/2$, further H-units with input pair separations $\Delta\theta > \lambda/2$ are introduced ($\Delta\theta \leqq \theta$). These by the Reichardt system give negative outputs. Thus, for $\theta > \lambda/2$, the total response consists of contradictory elements, (positive elements implying the true pattern direction, and negative elements implying the opposite to true pattern direction). If we make the simplest assumption that the H-unit outputs remain distinct, then the above situation is one which would give rise to the observed characteristics of the stationary stroboscopic effect (see Sec. 3.1).

c) The Dependence of f_l upon λ. We now show that the Reichardt scheme is consistent with the observed trends of the $f_l v.\ \lambda$ data.

The full expression for the sinewave response of the Reichardt multiplier shown in Fig. 6a is the following:

$$r = \frac{k \cdot \omega^2}{(a^2 + \omega^2)(b^2 + \omega^2)} \cdot \sin(2\pi \cdot \Delta\theta/\lambda) \qquad (3)$$

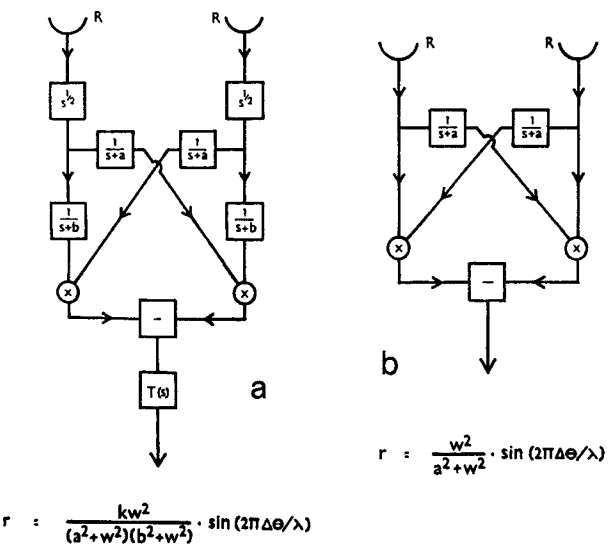

Fig. 6a and b. Complex frequency (s) domain representation of two, two-element motion detectors. In (a) is shown the full Reichardt scheme ($T(s)$ is a time-averaging element), and in (b) is shown Thorson's simplification of the Reichardt scheme. The sinewave response of each system is indicated

where a, b, and k are real positive constants. If the output, r, of the multiplier is held at some constant value then for $\omega \gg a, b$, we have:

$$\omega^2 = k' \cdot \sin(2\pi \cdot \Delta\theta/\lambda). \qquad (4)$$

For Thorson's simplification of the full Reichardt scheme (see Thorson, 1966, and Fig. 6b), we arrive at a similar expression.

$$\omega = k'' \cdot \sin(2\pi \cdot \Delta\theta/\lambda). \qquad (5)$$

Thus, it is seen that, at constant output, both versions of the multiplier imply an increase in temporal frequency with a decrease in spatial period. This is indeed the observed situation at constant (threshold) motion response (q. v. Fig. 2).

In view of the arguments (a), (b) and (c), above, we provisionally identify the H-unit with some form of Reichardt multiplier. [The phase sensitivity of the system is discussed in Sec. (b).] We also make the simplifying assumption that the filter characteristics of the H-units are independent of both θ and $\Delta\theta$.

4.3. Maximum Input Pair Separation, $\Delta\theta_{max}$

In Sec. 4.2b, it was proposed that the stationary stroboscopic effect arises from the presence of both positive and negative elements in the total motion response. Now, in order for the phenomenon to occur, θ must be large enough for H-units to be introduced with input pair separations, $\Delta\theta > \lambda/2$. Since $\lambda = 120°$ can give rise to the effect and $\lambda = 180°$ does not (see Fig. 2), it follows that the maximum angular input pair separation of the H-unit, $\Delta\theta_{max}$, must be greater than or equal to 120°/2 and less than 180°/2. That is, $60° \leqq \Delta\theta_{max} < 90°$.

This is discussed further in Sec. 5.3b.

4.4. Summation/Threshold Units

In this section we examine the interaction of H-unit outputs and V-unit outputs in terms of summation/threshold mechanisms.

In the case of the V-units, it has been proposed that the parameter, θ, be shifted from the V-unit to the associated threshold unit. With the data available it is not possible to distinguish between individual threshold shifts and output summation effects in the variation of $f_u v.\ \theta$. Two alternative schemes are shown in Fig. 7.

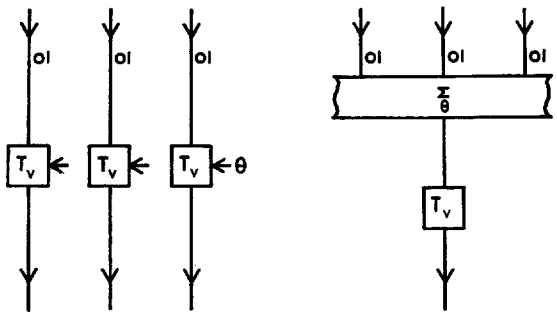

Fig. 7a and b. Two possible V-unit summation/threshold systems. In (a), each channel remains distinct, with each threshold unit T_V, a function of θ. In (b), all channels first feed into the (spatially) phase-independent summer, $\sum_\theta$; this then feeds into the single (θ-independent) threshold unit, T_V

In Fig. 7a, the $O1$-channels retain their distinctness. Each channel has an associated threshold unit, T_V, with θ as a parameter. In Fig. 7b, the $O1$-channels first feed (via some weighting function) into the summer, $\sum_\theta$. The single output of $\sum_\theta$ then feeds into a single threshold unit, T_V (which does not have θ as a parameter). Providing the summer, $\sum_\theta$, is spatially phase insensitive in operation (q. v. Sec. 4.1), both schemes are equally valid representations of this portion of the system.

We now study the H-unit summation/threshold system.

In proposing the origin of the stationary stroboscopic effect (see 4.2b) it was suggested that all H-unit outputs remain distinct, thus preserving positive and negative components in the total response. However, the sign of any H-unit output depends only upon the input pair separation, $\Delta\theta$ (see Sec. 4.2b), and therefore the above statement applies solely to H-units with different $\Delta\theta$. For H-units with identical $\Delta\theta$, there is no such restriction, and the same two possibilities exist for output interaction as do for the V-units.

Thus, in Fig. 8a, the $O2$-channels, retain their distinctness, even within a set from identical H-unit $\Delta\theta$. Each channel, independent of $\Delta\theta$ origin, has an associated threshold unit, T_H which has θ as a parameter. Alternatively, in Fig. 8b, the $O2$-channels from H-units with identical $\Delta\theta$ feed (via some weighting function) into the (spatially phase-insensitive) summer, $\sum_\theta^{\Delta\theta}$. In turn, the single outputs from each $\sum_\theta^{\Delta\theta}$ feed into single associated threshold units T_H (which do not have θ as a parameter).

The effect of relative variations in H-unit population with variations in $\Delta\theta$ is discussed later.

5. Detailed Analysis

In the following sections, the V-unit and the associated summation/threshold unit are given specific descriptions. A representation of the general motion response of the system is established and a motion threshold condition derived from this. By restricting the range over which this motion threshold condition

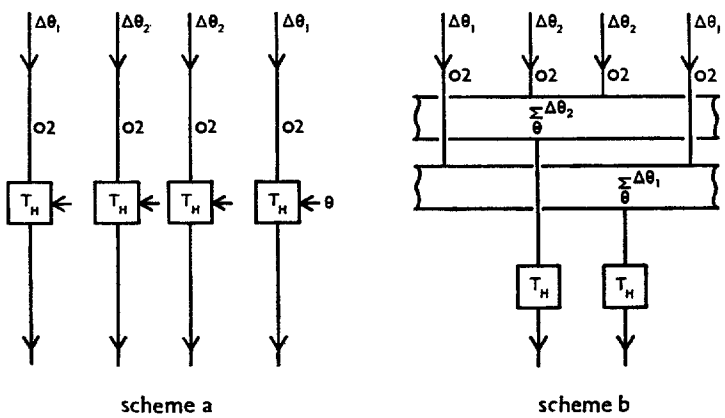

Fig. 8a and b. Two possible H-unit summation/threshold systems. In (a), each channel independent of $\Delta\theta$ origin has an associated threshold unit, T_H, which is sensitive to variations in θ. In (b), all outputs from H-units with identical $\Delta\theta$ first undergo (spatially) phase-independent summation in associated units, $\sum_\theta^{\Delta\theta}$; these then feed into single (θ-independent) threshold units, T_H

is applied, we deduce the detailed structure of the H-unit and derive the forms of associated total and relative population weighting factors.

It is shown necessary to modify the chosen Reichardt scheme in order that both the square and sine wave motion response data be fitted. It is further demonstrated that this modification changes the function performed by the system to that of running autocorrelation.

5.1. A Full description of the V-Unit and Associated Summation/Threshold System

Here, we obtain a specific description of the V-unit attenuation characteristics, and determine the sensitivity of the associated summation/threshold system to variations in the number of V-units in operation.

We first derive the V-unit transfer function.

In Sec. 4.2, it was suggested that the location of the parameter θ, be displaced from the V-unit to the summation/threshold unit. To obtain, from the experimental data, the resulting θ-independent attenuation characteristics of the V-unit, the following procedure was carried out.

Each of the de Lange attenuation characteristics, obtained at a different θ (q. v. Fig. 4) is shifted vertically to set the attenuation equal to zero at low (tending to zero) frequencies, and the curves then superimposed. The "averaged" attenuation characteristics thus obtained $W(\omega)$ say, are shown in Fig. 9.

It is seen that there is some spread in the data values defining $W(\omega)$, but the low pass form is evident. The response characteristics are flat at low frequencies, and significant attenuation does not commence until the temporal frequency exceeds 9.0 cps.

Note. The phase shift characteristics of the V-unit are not available. This does not necessarily limit the system description, since both the threshold flicker response and the threshold (sinewave) motion response are independent of any phase shift induced by the V-unit (see Forsyth, 1960; Foster, 1970a). For simplicity we treat the V-unit as a pure attenuator, with transfer function $W(\omega)$, and implicitly incorporate any phase shift factor into the H-unit description.

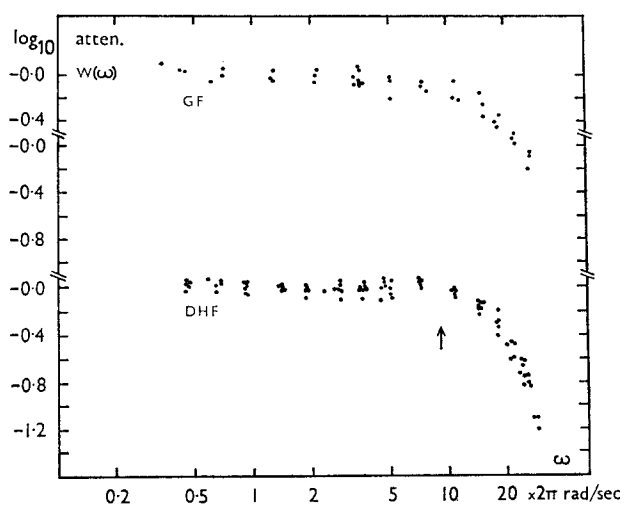

Fig. 9. The θ-independent, averaged, V-unit attenuation characteristics, $W(\omega)$

We now examine the V-unit summation/threshold system.

In Sec. 4.4, two possible types of summation/threshold system for the V-unit outputs were distinguished, viz., (a) in which all $O1$-channels are distinct, and (b) in which the $O1$-channels undergo phase independent summation (see Fig. 7). With reference to scheme (a), let the sensitivity of each threshold T_V, to variations in the V-unit population (caused by variations in θ) be described by $[P_V(\theta)]^{-1}$. That is, if a is the amplitude of the signal in the $O1$-channel, when $f=f_u$, then:

$$a=T_V \cdot [P_V(\theta)]^{-1}. \tag{6}$$

With reference to scheme (b), let each $O1$-channel feeding into the summer $\sum_\theta$ be weighted by $P'_V(\theta)$. That is, when $f=f_u$, we have (remembering that $\sum_\theta$ is spatially phase insensitive):

$$\theta \cdot P'_V(\theta) \cdot a = T_V \tag{7}$$

where θ gives a measure of the total number of outputs contributing. For the two schemes to be equivalent, we require the following equality to hold:

$$P_V(\theta) = \theta \cdot P'_V(\theta). \tag{8}$$

Thus, when $P_V(\theta)$ is specified experimentally, so is $P'_V(\theta)$. Therefore, in the remaining discussion, we refer solely to $P_V(\theta)$.

Now, $P_V(\theta)$ may be obtained from the curves of Fig. 4 by plotting attenuation at the lowest temporal frequency ($f_u=0.45$ c.p.s.) as a function of θ. This method only yields six points defining $P_V(\theta)$, and each is taken from an independently determined curve. In order to obtain a more precise definition of $P_V(\theta)$, direct measurement of flicker threshold as a function of θ (at $f_u=0.45$ c.p.s.) was carried out. The same experimental technique was used as in the determination of the de Lange attenuation characteristics described in Sec. 3.3.

The results of these measurements are displayed in Fig. 10. It may be seen that on a log-log plot, $P_V(\theta)$ may be described by two linear sections, with gradients $c_1 \simeq 0.7$ and $c_2 \simeq 0.3$, and with break at $\theta \simeq 90°$.

5.2. The General Motion Response $\mathscr{R}$, and Motion Threshold Condition

In order to procede with the specification of the H-unit and associated summation/threshold unit, it is necessary to establish an explicit representation of

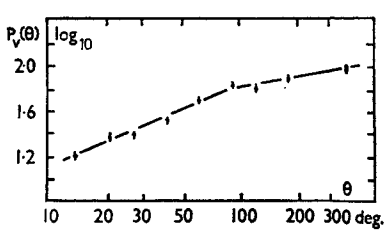

Fig. 10. The areal sensitivity, $P_V(\theta)$, of the V-unit summation/threshold system. The r.m.s. deviation associated with each point is indicated

the total motion response of the system, and derive an appropriate motion threshold statement. This we now do.

In Sec. 4.4, we discussed two possible types of summation/threshold mechanism for H-units of identical input pair separation $\Delta\theta$. Associated with each mechanism, an areal weighting factor may be introduced (q. v. Sec. 5.1) to describe the sensitivity of the system to the number of H-units in operation (the latter determined by θ). If these factors are $P_H(\theta)$ and $P'_H(\theta)$, then, as with the V-unit summation/threshold system, we may show that for equivalence of the two schemes, $P_H(\theta) = \theta \cdot P'_H(\theta)$. Hereafter, we refer solely to $P_H(\theta)$.

Now $P_H(\theta)$ is associated with the total H-unit population. There also exists the possibility that there are relative variations in the H-unit population with variations in input pair separation, $\Delta\theta$. Let this relative weighting be described by the function $p_H(\Delta\theta)$. That is, if the response of a single H-unit to some waveform is $r_{\omega\lambda}(\Delta\theta)$, and the final weighted response [of a single H-unit by scheme (a) of Fig. 8, or of a group of H-units by scheme (b) of Fig. 8] is $r'_{\theta\omega\lambda}(\Delta\theta)$, then:

$$r'_{\theta\omega\lambda}(\Delta\theta) = P_H(\theta) \cdot p_H(\Delta\theta) \cdot r_{\omega\lambda}(\Delta\theta). \tag{9}$$

The final motion response of the system then consists of all those $r'_{\theta\omega\lambda}(\Delta\theta)$ large enough to surmount the associated thresholds, $T_H (T_H > 0)$.

Let this set of outputs be $\mathscr{R}$, then using conventional set-theoretic notation, we may write:

$$\mathscr{R} = \{r'_{\theta\omega\lambda}(\Delta\theta) : \Delta\theta \in [\Delta\theta_{\min}, \Delta\theta_{\max}], \; |r'_{\theta\omega\lambda}(\Delta\theta)| > T_H\} \tag{10}$$

where $[\Delta\theta_{\min}, \Delta\theta_{\max}]$ is the set of all possible input pair separations, and $r'_{\theta\omega\lambda}(\Delta\theta)$ is defined by Eq. (9).

In order that $\mathscr{R}$ may give rise to a sensation of motion with well-defined direction, we require that $\mathscr{R}$ is non-empty, and, by the arguments of Sec. 4.2b, that all $r'_{\theta\omega\lambda}(\Delta\theta)$ have the same sign. (For simplicity this is chosen positive.)

Thus, for a sensation of well-defined directed motion to be elicited at some θ, ω, λ, the following must hold:

$$\mathscr{R} = \{r'_{\theta\omega\lambda}(\Delta\theta) : \Delta\theta \in [\Delta\theta_{\min}, \Delta\theta_{\max}], \; r'_{\theta\omega\lambda} > T_H\} \neq \phi \quad \text{(the empty set)}. \tag{11}$$

If the temporal (angular) frequency increases, $r_{\omega\lambda}(\Delta\theta)$, and therefore $r'_{\theta\omega\lambda}(\Delta\theta)$, decrease in magnitude (q. v. Sec. 4.2c). Since it is necessary that $r'_{\theta\omega\lambda}(\Delta\theta) > T_H$ for membership of $\mathscr{R}$, any increase in ω also implies a decrease in the population of $\mathscr{R}$. It then follows that the greatest frequency for which $\mathscr{R} \neq \phi$ is the lower critical frequency, $f_l (f = \omega/2\pi)$, (but see App. B).

For $r'_{\theta\omega\lambda}(\Delta\theta)$ all distinct, we need consider only one member of $\mathscr{R}$, viz: $r'_{\theta\omega\lambda}(\Delta\theta)_{\max}$. The latter is defined by the following expression:

$$r'_{\theta\omega\lambda}(\Delta\theta)_{\max} = \max\{r'_{\theta\omega\lambda}(\Delta\theta) : \Delta\theta \in [\Delta\theta_{\min}, \Delta\theta_{\max}], r'_{\theta\omega\lambda}(\Delta\theta) > 0\}. \tag{12}$$

Thus, for a sensation of well-defined directed motion to be just perceived, the following equality must be satisfied (see App. B):

$$\max\{P_H(\theta) \cdot p_H(\Delta\theta) \cdot r_{\omega\lambda}(\Delta\theta) : \Delta\theta \in [\Delta\theta_{\min}, \Delta\theta_{\max}], r_{\omega\lambda}(\Delta\theta) > 0\} = T_H. \tag{13}$$

The above is referred to as the motion threshold condition.

5.3. A Description of the H-Unit and Summation/Threshold System

In the following, it will be shown that by restricting, or holding constant, the values of θ, ω, and λ, the threshold statement of Eq. (13) may be simplified to expressions which may be applied directly to the observed data. By this method, we determine for the H-unit the most appropriate modification of Reichardt multiplier (and therefore define $r_{\omega\lambda}(\Delta\theta)$ for all input waveforms), and evaluate the two population weighting functions, $P_H(\theta)$ and $p_H(\Delta\theta)$.

a) The Choice of Reichardt Multiplier. In Sec. 4.2 it was demonstrated that the H-unit could be identified with some version of the Reichardt multiplicative interaction scheme. We now determine the most appropriate version.

The sinewave response of the H-unit can be expressed, generally, in the following form (see Sec. 4.2):

$$r_{\omega\lambda}(\Delta\theta) = G(\omega) \cdot \sin(2\pi \cdot \Delta\theta/\lambda) \tag{14}$$

where $G(\omega) = \frac{k\omega^2}{(a^2+\omega^2)(b^2+\omega^2)}$, if the full Reichardt scheme of Fig. 6a is used for the H-unit, or $G(\omega) = \frac{\omega}{a^2+\omega^2}$, if Thorson's simplification of Fig. 6b is adopted. $W(\omega)$, the V-unit attenuation factor (q. v. Sec. 5.1) may be omitted, since $W(\omega)$ is unity for $f < 9.0$ c.p.s. and for sinewave stimuli, $f_l < 9.0$ c.p.s. (see Fig. 2).

For $\omega \gg a, b$, Eq. (14) reduces to the following:

$$r_{\omega\lambda}(\Delta\theta) = \frac{1}{\omega^n} \cdot \sin(2\pi \cdot \Delta\theta/\lambda) \tag{15}$$

where $n = 2$ for the full Reichardt scheme, and $n = 1$ for Thorson's simplification. It may be shown that other modifications of the Reichardt scheme give different values of n. We use n to indicate which scheme is the most appropriate.

Consider values of $\Delta\theta \ll \lambda$. $\sin(2\pi\,\Delta\theta/\lambda)$ may be replaced by its argument, and the condition of $r_{\omega\lambda}(\Delta\theta) > 0$ may be dropped from the threshold statement of Eq. (13). Substituting for $r_{\omega\lambda}(\Delta\theta)$, Eq. (13) may thus be written:

$$\max\{P_H(\theta) \cdot p_H(\Delta\theta) \cdot (\omega^{-n} \cdot 2\pi\,\Delta\theta/\lambda) : \Delta\theta \in [\Delta\theta_{\min}, \Delta\theta_{\max}]\} = T_H. \tag{16}$$

The operation of taking the maximum is with respect to $\Delta\theta$, and the above therefore reduces to:

$$P_H(\theta) \cdot \omega^{-n} \cdot 2\pi/\lambda \cdot \max\{p_H(\Delta\theta) \cdot \Delta\theta : \Delta\theta \in [\Delta\theta_{\min}, \Delta\theta_{\max}]\} = T_H. \tag{17}$$

Now, $\max\{p_H(\Delta\theta) \cdot \Delta\theta : \Delta\theta \in [\Delta\theta_{\min}, \Delta\theta_{\max}]\}$ is not a function of ω or λ, and at fixed θ, $\max\{p_H(\Delta\theta) \cdot \Delta\theta : \Delta\theta \in [\Delta\theta_{\min}, \Delta\theta_{\max}]\}$ is constant. Let θ be fixed at $\theta_{\min}$ (the minimum area for which sensation of directed

motion may just be elicited), then, providing λ is not too small, the condition $\Delta\theta \ll \lambda$ is satisfied, since $\Delta\theta$ is restricted to the closed interval $[\Delta\theta_{\min}, \theta_{\min}]$ and $\theta_{\min} = 13°$. Furthermore, with θ constant, $P_H(\theta)$ is constant. Eq. (17) therefore simplifies to the following:

$$f_l^n = \text{constant}/\lambda. \tag{18}$$

This may be applied to the motion response data for:

i) Sine-wave stimuli ($r_{\omega\lambda}(\Delta\theta)$ is the sinewave response of the multiplier).

ii) $\theta = \theta_{\min}$.

iii) λ not too small (with respect to $\theta_{\min}$).

Most of the experimental data is for square wave stimuli (see Fig. 2). However, from the curves of Fig. 2a, displaying $f_l v.\ \theta, \lambda$, for both square and sinewave stimuli, it may be seen that for $f \simeq 1.0$ c.p.s., there is no significant difference in response form for the two stimulus waveforms. Therefore, for the purposes of this preliminary analysis, the square wave data (for $\lambda < 180°$) is treated as sinewave.

In Fig. 11, we have replotted on a log-log scale the observed $f_l v.\ \lambda$ response for intermediate values

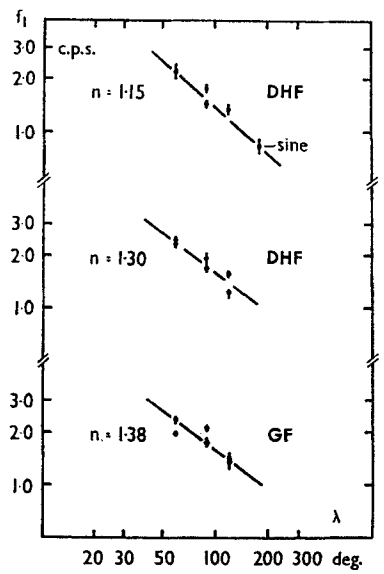

Fig. 11. The dependence of the lower critical frequency, f_l, upon spatial period, λ, at $\theta = \theta_{\min}$ (see text). Unless otherwise indicated, all data values are for square wave stimuli. The r.m.s. deviation associated with each point is marked

of λ with $\theta = \theta_{\min} = 13°$. It is seen that the gradients are closer to unity than any other integer, and in view of the elevation of the square wave response at large λ, we chose $n = 1$. Thus, Thorson's simplification of the Reichardt scheme is determined to be the most appropriate representation of the H-unit.

b) The General Form of the Relative Weighting Factor, $p_H(\Delta\theta)$. It was shown in Sec. 13 that there exists a maximum value to the input pair separation, $\Delta\theta$, viz. $\Delta\theta_{\max}$. Since $\Delta\theta_{\max}$ if finite, we have:

$$p_H(\Delta\theta) = 0, \quad \text{for} \quad \Delta\theta > \Delta\theta_{\max}. \tag{19}$$

Furthermore, since the $f_l v.\ \theta$ curves for $\lambda = 180°$ and 360° are monotonic (q. v. Fig. 2), it follows that $p_H(\lambda\theta)$ is also monotonic. From this and Eq. (19), we require $p_H(\Delta\theta)$ to decrease smoothly to zero. In practice we might chose something of the form:

$$\begin{aligned} p_H(\theta) &= \frac{1}{\Delta\theta^m}, \quad \text{for} \quad \Delta\theta \leqq \Delta\theta_{\max},\ m \gtrsim 1 \\ &= 0, \qquad \text{for} \quad \Delta\theta > \Delta_{\max}. \end{aligned} \tag{20}$$

It is shown in the next section that we need not be this specific in defining $p_H(\Delta\theta)$.

c) The Areal Weighting Factor, $P_H(\theta)$. We now deduce the form of the weighting function $P_H(\theta)$, associated with the total H-unit population.

Consider the threshold statement of Eq. (13). Substituting $p_H(\Delta\theta)$ defined by Eq. (20) and $r_{\omega\lambda}(\Delta\theta)$ by Eq. (14) into this expression, we obtain the following (for sinewave stimuli):

$$\max\left\{P_H(\theta)\cdot\Delta\theta^{-m}\cdot\frac{a}{a^2+\omega^2}\cdot\sin(2\pi\cdot\Delta\theta/\lambda) : \Delta\theta\in[\Delta\theta_{\min}, \Delta\theta_{\max}],\ \sin(2\pi\cdot\Delta\theta/\lambda)>0\right\} = T_H. \tag{21}$$

Now, $\Delta\theta_{\max} < 90°$ (q. v. Sec. 4.3), and therefore for $\lambda \geqq 180°$, the condition, $\sin(2\pi\cdot\Delta\theta/\lambda) > 0$, may be omitted from the above statement. We may also take out all those factors which do not contain $\Delta\theta$. This gives:

$$P_H(\theta)\cdot\frac{\omega}{a^2+\omega^2}\cdot\max\{\Delta\theta^{-m}\cdot\sin(2\pi\cdot\Delta\theta/\lambda) : \Delta\theta\in[\Delta\theta_{\min}, \Delta\theta_{\max}]\} = T_H. \tag{22}$$

But, $\max\{\Delta\theta^{-m}\cdot\sin(2\pi\cdot\Delta\theta/\lambda) : \Delta\theta\in[\Delta\theta_{\min}, \Delta\theta_{\max}]\} = \Delta\theta_{\min}^{-m}\cdot\sin(2\pi\cdot\Delta\theta_{\min}/\lambda)$ for $m \geqq 1$ [q. v. Eq. (20)], and this is true for all λ*. [It is noted that this simplification follows for any function $p_H(\Delta\theta)$ which falls off at least as rapidly as $(\sin\Delta\theta)^{-1}$.]

Assuming that $p_H(\Delta\theta)$ falls off at least as rapidly as $(\sin\Delta\theta)^{-1}$, Eq. (22) reduces to the following (for sinewave stimuli with $\lambda \geqq 180°$):

$$P_H(\theta)\cdot p_H(\Delta\theta_{\min})\cdot\sin(2\pi\cdot\Delta\theta_{\min}/\lambda)\cdot\frac{\omega}{a^2+\omega^2} = T_H. \tag{23}$$

In practice, only two values of $\lambda \geqq 180°$ are available, viz. 180° and 360° (q. v. Sec. 2). We show below that for $\lambda = 180°$, the rate constant a of Eq. (23) may be omitted.

It is observed (Figs. 2a, e) that with a sinewave stimulus of 360°, a directed motion response cannot be obtained for $\theta < 20°$. This is in contrast to the $\lambda = 180°$ case. We interpret this phenomenon in terms of Eq. (23) in the following way.

The LHS of Eq. (23) has a maximum value, with respect to ω, of

$$[P_H(\theta)\cdot p_H(\Delta\theta_{\min})\cdot\sin(2\pi\cdot\Delta\theta_{\min}/\lambda)\cdot(1/2a)].$$

If $P_H(\theta)$ is reduced to such a value that this expression is less than T_H, then Eq. (23) can no longer be satisfied and f_l cannot be defined. It is suggested that in the present case, with $\lambda = 360°$, the reduction in $P_H(\theta)$

* If we include H-units with input (receptor) pairs at angles ϕ to the direction of motion, then the expression in brackets becomes:

$$\max\{\Delta\theta^{-m}\cdot\sin(2\pi\cdot\Delta\theta\cdot\cos\phi/\lambda) : \Delta\theta\in[\Delta\theta_{\min}, \Delta\theta_{\max}], \phi\in[0, \pi]\}$$

assuming $p_H(\Delta\theta)$ is not a function of ϕ. This reduces to the simpler expression in the text (q.v. Introduction, Sec. 4).

for values of $\theta < 20°$ is such that the LHS of Eq. (23) is less than T_H, and at $\theta = 20°$, just equal to T_H. Accordingly, an approximate value of a is given by the value of f_l at $\theta = 20°$, $\lambda = 360°$.

From this, and general inspection of the sine response curves of Fig. 2 it is seen that a is only significant at low temporal frequencies, and may be neglected for the $\lambda = 180°$ response.

Thus, if the $\lambda = 180°$ response, only, is considered, Eq. (23) simplifies to the following:

$$P_H(\theta) = \text{constant } f_l(\theta). \tag{24}$$

That is, the $\lambda = 180°$, $f_l v.\ \theta$ sine response gives a direct measure of the areal (population) weighting function, $P_H(\theta)$.

It will be shown later that, analogously to $P_V(\theta)$, $P_H(\theta)$ may be described by the following function:

$$\begin{aligned} P_H(\theta) &= \theta^{c_1}, \quad \text{for} \quad \theta < \theta_b \\ &= k \cdot \theta^{c_2}, \quad \text{for} \quad \theta \geqq \theta_b,\ k = \theta_b^{(c_1 - c_2)}. \end{aligned} \tag{25}$$

To summarise, we have obtained for the H-unit the most appropriate version of Reichardt multiplier, fixed the general form of the relative (population) weighting factor, $p_H(\Delta\theta)$, and arrived at a description of the areal (population) weighting factor, $P_H(\theta)$. We now examine the fit of the model to the observed data.

The threshold statement of Eq. (23) may be simplified with the inclusion of $p_H(\Delta\theta)$ in the constant T_H. $P_H(\theta)$ may also be replaced by the expression of Eq. (25). This gives:

$$\theta^c \cdot \frac{\omega}{a^2 + \omega^2} \cdot \sin(2\pi \cdot \Delta\theta_{\min}/\lambda) = T_H,\ c = c_1 \text{ or } c_2 \tag{26}$$

which holds for all θ, providing $\lambda = 180°$ or $360°$. For this range of λ, variations in $\Delta\theta_{\min}$ ($\Delta\theta_{\min} \leqq \theta_{\min} = 13°$) are not significant in determining the relationship of one curve with respect to another. For the present, we assign an arbitrary value to $\Delta\theta_{\min}$ (less than 13°) and determine a specific value later.

Eq. (26) was fitted to the $f_l v.\ \theta$ sine data of Fig. 2. The results obtained are displayed in Fig. 12 and the final values of the parameters indicated.

The significance of the rate constant a is evident at low θ, in that the $\lambda = 360°$ f_l response is depressed in relation to the 180° response. It is also noted that $P_H(\theta)$ defined by Eq. (25) provides an adequate description of the $f_l v.\ \theta$ dependence.

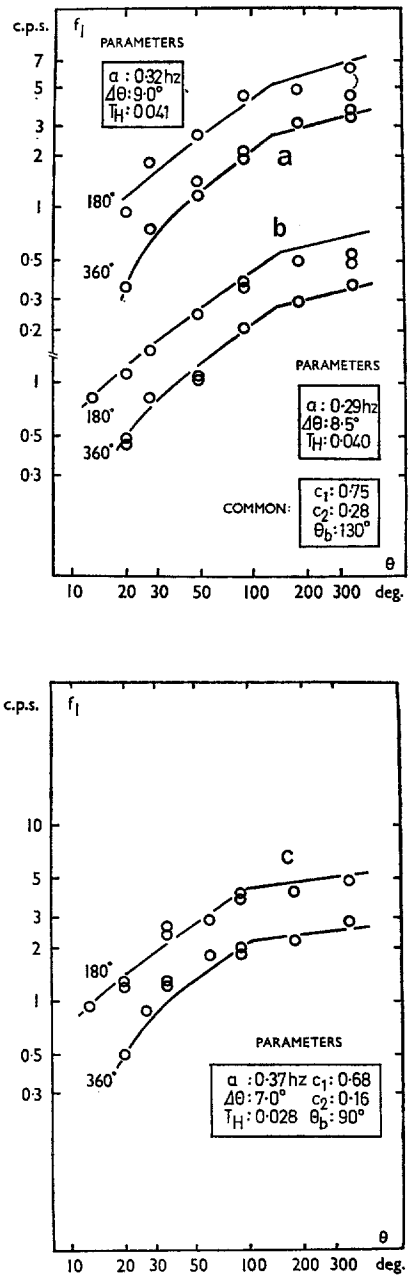

Fig. 12a–c. The $f_l v.\ \theta, \lambda$ sinewave response of the model compared with the experimental sinewave data. (a) and (b) show theoretical fits to the sinewave data of Figs. 2d and 2a respectively, and (c) shows the theoretical fit to the sinewave data of Fig. 2e. The relevant parameter values are indicated in each case

5.4. A Revised Description of the H-Unit

We examine here the ability of the proposed scheme to provide a description of the square-wave motion-threshold response data. It will be shown necessary to extend the threshold statement of Eq. (13), and to modify the representation of the H-unit by Thorson's simplification of the Reichardt scheme.

In Sec. 5.2 it was shown that in order for a sensation of well-defined directed motion to be just elicited, the following (motion-threshold) statement must hold:

$$\begin{aligned} &\max\{P_H(\theta) \cdot p_H(\Delta\theta) \cdot r_{\omega\lambda}(\Delta\theta) \\ &\quad : \Delta\theta \in [\Delta\theta_{\min}, \Delta\theta_{\max}], r_{\omega\lambda}(\Delta\theta) > 0\} = T_H. \end{aligned} \tag{27}$$

Providing the relative weighting factor, $p_H(\Delta\theta)$, falls off at least as rapidly as $(\sin\Delta\theta)^{-1}$, then the above reduces to the expression of Eq. (26), describing the sinewave $f_l v.\ \theta, \lambda$ motion response. A description of the population weighting function, $P_H(\theta)$, is also obtained.

In order to arrive at a description of the square wave data, an expression for the H-unit square wave response must first be derived. This is then inserted in the above. The steady-state response of Thorson's scheme to a square wave train of unit amplitude, is given (Foster, 1970a) by the following [V-unit

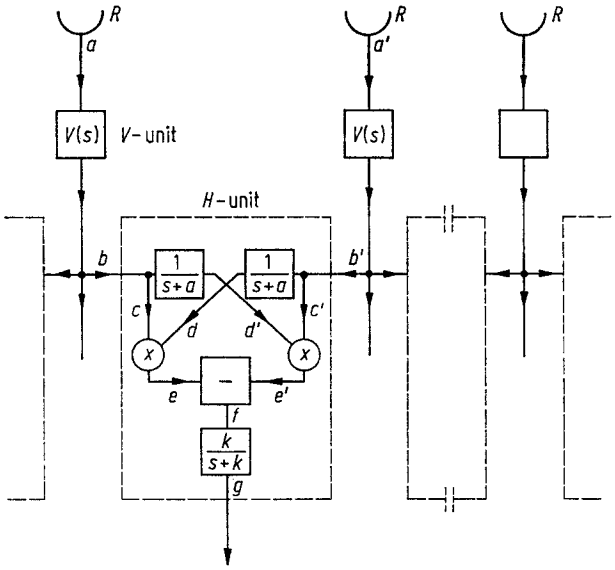

Fig. 13. Representation of the complete model in the complex frequency (s) domain (see text)

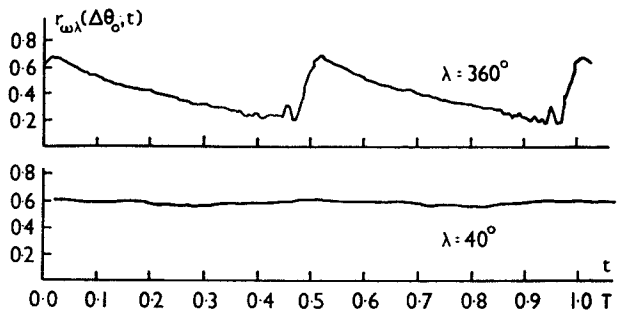

Fig. 14. The variation of the H-unit square wave response, $r_{\omega\lambda}(\Delta\theta_0, t)$ with time, t, (t in units of the period, T) at fixed $\Delta\theta_0$. For $\lambda = 360°$, $f = 0.7$ hz, and for $\lambda = 40°$, $f = 3$ hz; the rate constant $a = 0.32$ hz, and $k = 0.6$ hz

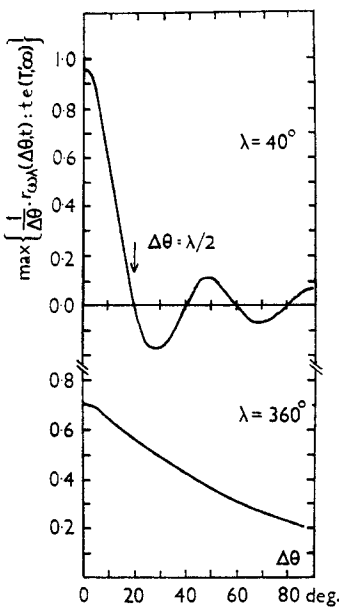

Fig. 15. The variation of the maximum H-unit output with respect to time, i. e. $\max\left\{\frac{1}{\Delta\theta}\cdot r_{\omega\lambda}(\Delta\theta, t): t\in(T', \infty)\right\}$, with input pair separation, $\Delta\theta$. For $\lambda = 40°$, $f = 3$ hz, and for $\lambda = 360°$, $f = 0.7$ hz; the rate constant, $a = 0.32$ hz, and $k = 0.6$ hz

attenuation, $W(\omega)$, included]:

$$r_{\omega\lambda}(\Delta\theta, t) = \sum_{\substack{n \\ \text{odd} \\ +1}}^{+\infty}\sum_{n'} W(n\omega)\,W(n'\omega) \cdot \frac{16\omega}{\pi^2}\left[\frac{\cos\omega n' t\cdot\sin\omega n(t+\Delta t)}{n(a^2+\omega^2 n'^2)} - \frac{\sin\omega n' t\cdot\cos\omega n(t+\Delta t)}{n'(a^2+\omega^2 n^2)} - \frac{a\omega\cdot\sin\omega n' t\cdot\sin\omega n(t+\Delta t)}{(a^2+\omega^2 n^2)\cdot(a^2+\omega^2 m'^2)}\cdot\left[\frac{n}{n'} - \frac{n'}{n}\right]\right]. \quad (28)$$

It is noted that the response is time-dependent even in the steady state, in contrast to the sinewave response [q. v. Eq. (1)].

If the threshold statement of Eq. (13) is rederived from the general motion response, [Eq. (11)], with the H-unit response now as a function of both $\Delta\theta$ and t, the following extended condition is obtained:

$$\max\{P_H(\theta)\cdot p_H(\Delta\theta)\cdot r_{\omega\lambda}(\Delta\theta, t): \Delta\theta\in[\Delta\theta_{\min}, \Delta\theta_{\max}], t\in(T', \infty), r_{\omega\lambda}(\Delta\theta, t) > 0\} = T_H \quad (29)$$

where (T', ∞), $T' \gg 1/a$, is the time for which the steady-state response only, need be considered.

If $r_{\omega\lambda}(\Delta\theta, t)$, defined by Eq. (28), is substituted into the above expression, and the maximum evaluated with respect to both $\Delta\theta$ and t, it is found that the values of f_l predicted are considerably in excess of these recorded. That is, the model in its present form, with Thorson's simplification of the Reichardt scheme for the H-unit, does not yield a true description of the observed square-wave response data, although the sinewave data may certainly be fitted.

In order to reduce the significance of the higher harmonics, without affecting the response to the fundamental, we introduce into the H-unit output a low pass filter with transfer function:

$$X(s) = \frac{k}{s+k} \quad (30)$$

where s is the complex frequency, and k is a real positive constant. Such a filter attenuates the time-varying component of the output, only, and this leaves the sinewave response intact.

In Fig. 13 we show the full scheme with this new modification incorporated.

Note: The introduction of this output filter modifies the function performed by the system to include the operation of *running* autocorrelation (q. v. Licklider, 1951, and App. C). This contrasts with the operation of "straight" autocorrelation carried out by the basic Reichardt scheme (Reichardt and Varju, 1959).

If we now rederive the steady-state square-wave response of a single H-unit (q. v. App. D) we obtain the following:

$$r_{\omega\lambda}(\Delta\theta, t) = \sum_{\substack{n \\ \text{odd} \\ -\infty}}^{+\infty}\sum_{n'} \frac{4}{\pi^2}\cdot\frac{e^{jn2\pi\cdot\Delta\theta/\lambda}}{nn'}\cdot\left[\frac{1}{a+jn\omega} - \frac{1}{a+jn'\omega}\right] \cdot e^{j\omega(n+n')t}\cdot\frac{k}{k+j(n+n')\omega}\cdot W(n\omega)\,W(n'\omega) \quad (31)$$

which may now be inserted into the threshold statement of Eq. (29).

In order to determine the maximum of $p_H(\Delta\theta) \cdot r_{\omega\lambda}(\Delta\theta, t)$, with respect to $\Delta\theta$ and t, [q. v. Eq. (29)], we must first find the conditions under which the requirement $r_{\omega\lambda}(\Delta\theta, t) > 0$ is satisfied.

In Fig. 14 is shown the variation of $r_{\omega\lambda}(\Delta\theta, t)$ with t, at fixed $\Delta\theta$, for two values of λ, viz: 40° and 360°. In Fig. 15 is shown the variation of

$$\max\left\{\frac{1}{\Delta\theta} \cdot r_{\omega\lambda}(\Delta\theta, t) : t \in (T', \infty)\right\}$$

with $\Delta\theta$, also for these two λ values.

It is seen that the following two conditions are satisfied:

i) For $\lambda \geqq 180°$, $r_{\omega\lambda}(\Delta\theta, t) > 0$ for all $\Delta\theta$, and for $\lambda < 180°$, $r_{\omega\lambda}(\Delta\theta, t) > 0$ for $\Delta\theta < \lambda/2$.

ii) For $m \geqq 1$, $\Delta\theta = \Delta\theta_{\min}$ yields a maximum of $[\Delta\theta^{-m} \cdot r_{\omega\lambda}(\Delta\theta, t)]$ with respect to $\Delta\theta$.

It is possible to prove (Foster, 1970a) that these two statements are true for a first approximation to expression (31) defining $r_{\omega\lambda}(\Delta\theta, t)$. It is noted that (i) is consistent with the observed conditions for the stationary stroboscopic effect (q. v. Sec. 3) and that (ii) is also true for the sinewave case (q. v. Sec. 5.3c).

Substituting $r_{\omega\lambda}(\Delta\theta, t)$ defined by Eq. (31), and $P_H(\theta)$ defined by Eq. (25), into the threshold statement of Eq. (29), we obtain the following relationship between the input variables:

$$\theta = \exp\left[\frac{1}{c_1} \cdot \ln\left\{T_H \Big/ \frac{1}{\Delta\theta_{\min}} \cdot r_{\omega\lambda}(\Delta\theta_{\min}, t)_{\max}\right\}\right] \quad \text{for} \quad \theta < \theta_b \qquad (32)$$

$$= \exp\left[\frac{1}{c_2} \cdot \ln\left\{T_H \Big/ \frac{1}{\Delta\theta_{\min}} \cdot r_{\omega\lambda}(\Delta\theta_{\min}, t)_{\max} \cdot \theta_b^{(c_2 - c_1)}\right\}\right] \quad \text{for} \quad \theta \geqq \theta_b$$

providing that if $\lambda < 180°$, $\theta < \lambda/2$. The subscript max is with respect to time.

Values for the constants a, T_H, θ_b, c_1 and c_2, obtained earlier (Sec. 5.3), were inserted into Eq. (32) and this was then fitted to the square wave data of Fig. 2 using trial values of k and $\Delta\theta_{\min}$ (k affects the low frequency end of the response and $\Delta\theta_{\min}$, the small λ end of the response). The theoretical fit to the data, and optimum parameter values, are displayed in Fig. 16.

In Fig. 16a, the theoretical fit to the sine and square wave data of Fig. 2a is shown, for $\lambda = 180°$ and 360°. In Fig. 16b, the fit to the data of Fig. 2c, e is shown, also for $\lambda = 180°$ and 360°. In Fig. 16c is shown the theoretical fit to the square wave data of Fig. 2b for all experimental values of λ.

The elevation of the square wave response with respect to the sinewave response, at low temporal frequencies, is evident.

6. *Predictions of the Model*

We now obtain predictions from the model concerning the behavior of the real system, and then subject these predictions to experimental test. The particular property that is investigated is the phase sensitivity of the model (and the system) to variations in the phase structure of the stimulus pattern (q. v. Reichardt and Varju, 1959).

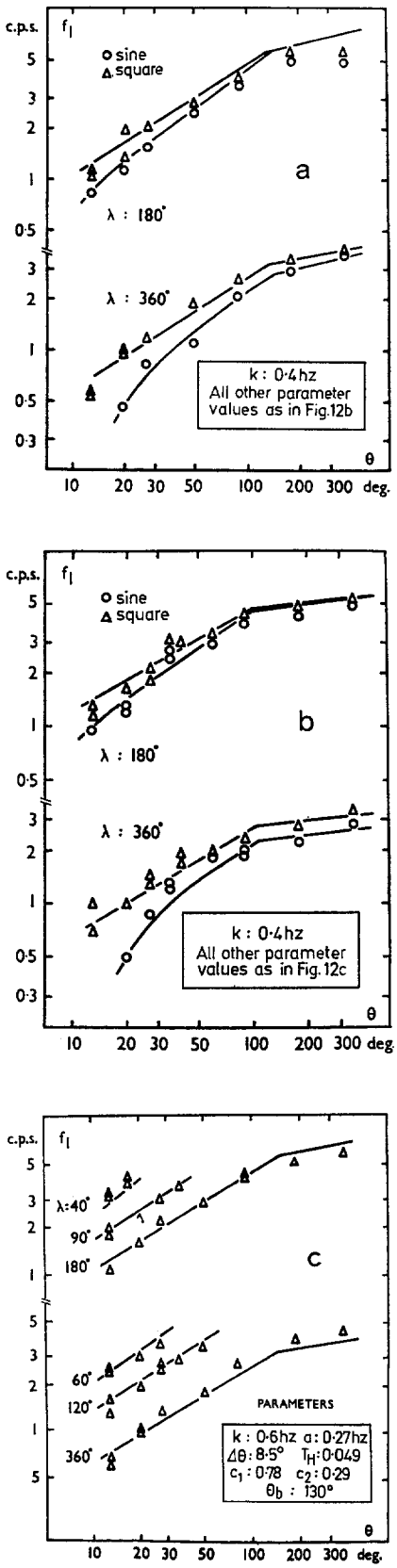

Fig. 16a–c. The $f_l v.\ \theta, \lambda$ square wave response of the model compared with the experimental squarewave data. In (a) is shown the theoretical fit to the sine and square wave data of Fig. 2a; in (b) is shown the theoretical fit to the square wave data of Fig. 2c and to the sinewave data of Fig. 2e; in (c) is shown the theoretical fit to the square wave data of Fig. 2b. The relevant parameter values are indicated in each case

6.1. The Phase Sensitivity of the H-Unit Response

We first determine the response of the H-unit to a general, moving spatially-periodic waveform. Let the fixed-point time-varying course of this signal be described by $f(t)$ with period T.

Referring to Fig. 13, showing the full model, let $f(t)$ be incident at input (a) and $f(t+\Delta t)$ be incident at input (a'). Let $F(s)$ be the Laplace transform of $f(t)$, and $R(s)$ be the Laplace transform of the final response, $r_{\omega\lambda}(\Delta\theta, t)$. Following the signals through the system, we obtain the relationship below:

$$R(s) = \left[\left\{F(s) * F(s)\cdot\frac{e^{s\Delta t}}{s+a}\right\} - \left\{F(s)\cdot\frac{F(s)}{s+a} * F(s)\cdot e^{s\Delta t}\right\}\right]\cdot\frac{k}{s+k} \tag{33}$$

where * represents the operation of convolution. (The attenuation due to the V-units is omitted.)

Performing the convolution, and inverting back into the time-domain, we arrive at the following expression for the steady-state response:

$$r_{\omega\lambda}(\Delta\theta, t) = \sum_{n}^{+\infty}\sum_{m}^{+\infty}\frac{\omega^2}{4\pi^2}\cdot e^{j\omega n\Delta t}\cdot e^{j\omega(n+m)t} \cdot\left[\frac{1}{a+j\omega n}-\frac{1}{a+j\omega m}\right]\cdot\frac{k}{k+j\omega(n+m)} \cdot F_0(j\omega n)F_0(j\omega m) \tag{34}$$

with

$$F_0(j\omega n) = \int_0^T f(t)\cdot e^{-j\omega nt}\,dt.$$

If we write $F_0(j\omega n) = |F_0(j\omega n)|\cdot e^{j\phi(\omega n)}$, where $\phi(\omega n)$ is the phase structure of the stimulus pattern, then $F_0(-j\omega n) = |F_0(j\omega n)|\cdot e^{-j\phi(\omega n)}$. Substituting in Eq. (34), we see that those terms of the double sum with $n = -m$ are independent of the phase structure of the stimulus pattern, whereas those terms with $n \neq -m$ are *not* independent of the phase structure of the stimulus pattern. (It will also be noted that $n = -m$ implies time-invariance, and $n \neq -m$ implies time-dependence.)

It may also be shown (Foster, 1970a) that attenuation by the factor

$$\left\{\left[\frac{1}{a+jn}-\frac{1}{a+jm}\right]\cdot\frac{k}{k+j(n+m)}\right\}$$

in Eq. (34) is such that $m \neq -n$ only gives rise to significant contributions to the total motion response when ω is low. At high ω, the dominant term of the summand is that with $m = -n = \pm 1$.

We therefore have the following:

i) At low ω, the response of the model depends upon the phase structure of the stimulus pattern. At high ω it does not.

From Eq. (32) it is seen that large ω implies large θ (at constant [threshold] motion response), and small ω implies small θ. Thus (i) may be re-written:

ii) At small θ, the response of the model depends upon the phase structure of the stimulus pattern. At large θ, it does not.

This property of the model, i. e., (i) [or (ii)] is directly attributable to the presence of the output filter, $k/(s+k)$, and contrasts with the universal phase insensitivity of the original Reichardt scheme (Fig. 6a).

6.2. The Phase Sensitivity of the System

We now determine whether the system exhibits the frequency-dependent phase sensitivity predicted by (ii). The experimental technique adopted is described below.

A radial grating with the waveform shown in Fig. 17 was substituted for the conventional square wave type. This grating consists of two elements, (ab) and (cd), of fixed angular subtenses $X/3$ and $X/6$ respectively, and variable angular separation, Δx. By varying Δx, we vary the magnitude and phase

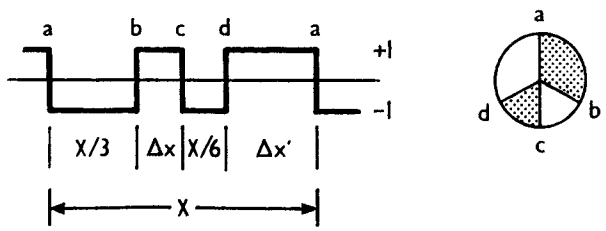

Fig. 17. The waveform and grating used in the phase sensitivity test (q. v. Sec. 6.2). The two sectors, ab and cd have fixed angular subtenses; their angular separation, bc is variable

of the Fourier components making up the stimulus pattern. If $F(nv)$ is the Fourier transform the waveform, we have the following for $|F(nv)|^2$:

$$|F(nv)|^2 = \frac{2}{\pi^2 n^2}[2 - \cos(2\pi n/3) - \cos(vn\Delta x) - \cos(vn\Delta x') + \cos(2\pi n/3 + vn\Delta x) + \cos(2\pi n/3 + vn\Delta x') - \cos\{2\pi n/3 + vn(\Delta x + \Delta x')\}] \tag{35}$$

where $v = 2\pi/X$.

It may be seen that interchange of Δx and $\Delta x'$ leaves $|F(nv)|^2$ unaltered; i. e., $|F(nv)|$ is a symmetric function of Δx (or $\Delta x'$), about the point $\Delta x = \Delta x' = 90°$.

Thus, if the system is insensitive to the phase structure of the stimulus pattern, i. e., operates on $|F(nv)|$, then the response should by a symmetric function of the shift variable Δx (or $\Delta x'$). Alternatively, if the system is insensitive to the phase structure of the stimulus pattern, then the response should be an asymmetric function of Δx (or $\Delta x'$).

To determine, then, whether the symmetry of the response depends on θ in the manner predicted by (ii), the following experiment was performed.

The lower critical frequency, f_l was measured as a function of the shift variable, Δx, at two extreme values of θ, viz: 17° and 360°. Readings were taken in pairs, i. e., $f_l(\Delta x)$ and $f_l(90° - \Delta x)$, and the ordering reversed periodically to offset the presence of systematic drifts. Two naive observers were used as subjects.

In Fig. 18 the quotient of each pair of readings, $f_l(90° - \Delta x)/f_l(\Delta x)$, is plotted as a function of Δx for each value of θ (the s. d. is indicated). For both subjects, it is seen that at $\theta = 360°$, $f_l(90° - \Delta x)/f_l(\Delta x)$ remains close to unity, whereas, for $\theta = 17°$, there are sharp departures from unity.

In view of the earlier discussion, it follows that at small θ, the system exhibits sensitivity to the phase structure of the stimulus, and at large θ, insensitivity to the phase structure of the stimulus. Predictions (i) and (ii) are therefore verified.

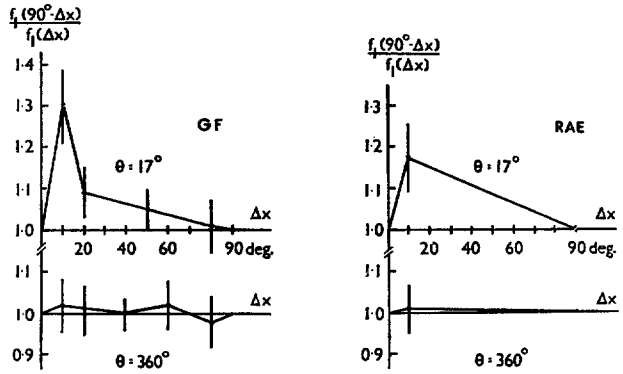

Fig. 18. The quotient of paired values of f_l as a function of the shift variable x, at two values of θ. The r.m.s. deviation associated with each point is indicated

7. Conclusion

In line with the stated intention, we have constructed a functional model of the human visual system in its response to a certain class of moving stimuli. In order to demonstrate the validity of this representation, we obtained predictions from the model concerning the phase sensitivity of the system, and then verified these predictions experimentally.

It is noted that the frequency dependence of the model's phase sensitivity arises from the presence of the low pass output filter. This filter also modifies the function performed by the model to include that of running autocorrelation. It is emphasised, however, that the filter was introduced in order to reconcile the square-wave motion response with the sinewave.

As a final comment, it is pointed out that the range of validity of the model is restricted to the class of input stimuli defined, and need not necessarily extend beyond this range.

Appendix A

Small-Signal Linearity

Let the response of some non-linear element to an input x be $f(x)$, and suppose $f(x)$ and all of its derivatives exist in the open interval (x_0-a, x_0+a). Providing $\Delta x<a$, we may expand $f(x_0+\Delta x)$ in a Taylor's Series thus:

$$f(x_0+\Delta x)=f(x_0)+\Delta x\cdot f'(x_0)+\frac{(\Delta x)^2}{2!}\cdot f''(x_0)+\text{higher terms}. \quad (A.1)$$

If Δx is sufficiently small, then (A. 1) reduces to:

$$f(x_0+\Delta x)=f(x_0)+\Delta x\cdot f'(x_0) \quad (A.2)$$

i. e.,

$$\Delta f=\Delta x\cdot f'(x_0). \quad (A.3)$$

Thus, the element with characteristic $f(x)$ behaves linearly for small changes Δx changes in the input.

A non-linearity which satisfies the conditions on $f(x)$ (q. v. Spekreijse and Oosting, 1970) and which is relevant in this context of the human visual system (see de Lange, 1954; Veringa, 1958) is $\log x$. For this non-linearity, an error of less than ten per cent is introduced into the output if the linear approximation of Eq. (A. 3) is used with $\Delta x=0.1\,x_0$. Such an error is within experimental tolerances (q. v. Sec. 3), and accordingly for this restricted range of input amplitudes we treat the system as consisting of linear elements.

Appendix B

A Rigorous Definition of the Lower Critical Frequency

For a sensation of motion to be elicited, we require there to be at least one H-unit output, r', greater than the associated threshold, T_H, i. e., at least one $r'\in(T_H,\infty)$. The interval (T_H,∞) has the greatest lower bound T_H, but no minimal element. Since r' is a continuous function of f (and varies approximately inversely), it follows that there is a least upper bound to those f for which $r'>T_H$, but *no* maximal element f_l. Thus, strictly, the lower critical frequency f_l cannot be defined as the greatest frequency for which there exists some $r'>T_H$.

However, in practice, the system has a limited sensitivity; i. e., for each $r'_0\in(T_H,\infty)$, we may choose a $\delta>0$ such that for all $r'\in(r'_0-\delta/2, r'_0+\delta/2)$, the induced sensation of motion appears the same. In particular, we may choose a $\delta_0>0$, such that the latter is true for all $r'\in(T_H, T_H+\delta_0)$. If r' is defined to be a one-to-one function of f, g say, it them follows that we may write for this δ_0, the statement below:

$$f_l\in(g^{-1}(T_H+\delta_0), g^{-1}(T_H)).$$

By letting r' approach sufficiently close to T_H (maintaining $r'>T_H$), f_l may be specified with an arbitrarily small (but non-zero) error.

Thus although f_l cannot be defined rigorously as the greatest frequency for which $r'>T_H$, it is convenient abbreviation of the above expression. In the "limit" we write:

$$g^{-1}(r')=f_l, \quad \text{when} \quad r'=T_H.$$

Appendix C

To show that the Model Performs the Operation of Running Autocorrelation

We work in the time-domain. Referring to Fig. 13, let time-varying signals, $f_1(t)$ and $f_2(t)=f_1(t-\Delta t)$, be incident at the inputs (b) and (b') of the H-unit. After passage through the cross-filter, $f_2(t)$ transforms to $f'_2(t)$, thus:

$$f'_2(t)=\int_0^t f_2(t-\xi)\cdot e^{-a\xi}d\xi. \quad (C.1)$$

On the LHS of the system, we have after multiplication:

$$f_1(t)\cdot\int_0^t f_2(t-\xi)\cdot e^{-a\xi}d\xi \quad (C.2)$$

and this, after transmission through the output filter, yields:

$$\int_0^t e^{-k(t-t')}\cdot\left[f_1(t')\cdot\int_0^{t'} f_2(t'-\xi)\cdot e^{-a\xi}d\xi\right]dt'. \quad (C.3)$$

(A similar result is obtained for the RHS of the model.)

Rearranging (C. 3) and putting $(t-t')=\eta$, we have:

$$\int_0^t e^{-a\xi}\left[\int_0^{t-\xi} e^{-k\eta}\cdot f_1(t-\eta)\cdot f_2(t-\eta-\xi)\,d\eta\right]d\xi. \quad (C.4)$$

The integrand of (C. 4) is large when ξ and η are small. We also require t large (tending to infinity) in order to achieve steady state. The upper limits on both integrals may therefore be extended to infinity. That is, to a good approximation, Eq. (C. 4) becomes:

$$\int_0^\infty e^{-a\xi}\left[\int_0^\infty e^{-k\eta}\cdot f_1(t-\eta)\cdot f_2(t-\eta-\xi)\,d\eta\right]d\xi. \quad (C.5)$$

The expression in brackets [ ] is the running crosscorrelation function between $f_1(t)$ and $f_2(t-\xi)$. If $f_2(t)$ is replaced by $f_1(t-\Delta t)$, we obtain Licklider's running autocorrelation function $\phi_{\mathrm{RACF}}(t, T)$ (see Licklider, 1951), where

$$\phi_{\mathrm{RACF}}(t, T)=\int_0^\infty w(t')\cdot f(t-t')\cdot f(t-T-t')\,dt'. \quad (C.6)$$

Here, $T=\Delta t+\xi$, and $w(t')=e^{-kt'}$.

This may be contrasted with the "straight" autocorrelation function $\phi_{ACF}(T)$ implied by the original Reichardt scheme:

$$\phi_{ACF}(T) = \lim_{\mu\to\infty} \frac{1}{\mu} \int_{-\mu/2}^{+\mu/2} f(t)\cdot f(t+T)\,dt. \qquad (C.7)$$

Appendix D

The Steady-State Squarewave Response of the Modified H-Unit

Let $f(t)$ be a square wave of unit amplitude and period T, and let the Laplace transform of $f(t)$ be $F(s)$. Then,

$$F(s) = \frac{1}{s}\left[\frac{1-e^{-sT/2}}{1+e^{-sT/2}}\right]. \qquad (D.1)$$

Referring to Fig. 13, let $f(t)$ be incident at input (a) and $f(t+\Delta t)$ be incident at input (a'). Working in the complex frequency domain and following the signal through the system, we obtain the expression below for the intermediate output $R'(s)$ at the point (f):

$$R'(s) = \left\{[V(s)\cdot F(s)]^* \left[\frac{1}{s+a}\cdot e^{s\Delta t}\cdot F(s)\right]\right\} - \left\{\left[\frac{1}{s+a}\cdot V(s)\cdot F(s)\right]^* [V(s)\cdot e^{s\Delta t}\cdot F(s)]\right\} \qquad (D.2)$$

where * represents the operation of convolution, and $V(s)$ is the transfer function of the V-unit.

Substituting for $F(s)$, defined by (D. 1), and writing the convolution in full, we obtain:

$$R'(s) = \frac{1}{2\pi j}\int_{\sigma-j\infty}^{\sigma+j\infty} V(s')\cdot V(s-s')\cdot\frac{1}{s}\cdot\frac{1-e^{-s'T/2}}{1+e^{-s'T/2}} \cdot\frac{1}{s-s'}\cdot\frac{1-e^{-(s-s')T/2}}{1+e^{-(s-s')T/2}}\cdot e^{s\Delta t}\cdot\left[\frac{1}{s'+a}-\frac{1}{s-s'+a}\right]ds' \qquad (D.3)$$

where $0<\sigma<\mathrm{Re}(s)$.

The integrand of (D. 3) has the following singularities to the left of $s'=\sigma$:

i) A simple pole at $s'=0$.

ii) A simple pole at $s'=-a$.

iii) Singularities due to $V(s')$.

iv) Simple poles at $s'=j\omega n$, where $\omega=2\pi/T$ and n is odd.

The residue at $s'=0$ disappears on evaluation. The residue at $s'=-a$ gives rise to a term when inverted back into the time domain, falls of as e^{-at}. In the limit, as $t\to\infty$, this vanishes. (We want the steady state component of the response.) The singularities of $V(s)$ must all lie to the left of the imaginary axis, and these give rise to terms which also vanish at $t\to\infty$. Thus we are left with the residues at $s'=j\omega n$. That is:

$$R'(s) = \sum_{\substack{n\\ \text{odd}\\ -\infty}}^{+\infty} V(j\omega n)\cdot V(s-j\omega n)\cdot\frac{1}{j\omega n}\cdot\frac{2}{T/2}\cdot\frac{1}{s-j\omega n} \cdot\frac{1+e^{sT/2}}{1-e^{-sT/2}}\cdot e^{j\omega n\Delta t}\cdot\left[\frac{1}{j\omega n+a}-\frac{1}{s-j\omega n+a}\right]. \qquad (D.4)$$

Transmission of $R'(s)$ through the output filter $k/(s+k)$ (q. v. Fig. 13) and subsequent inversion back into the time domain yields the following contour integral for the final response $r_{\omega\lambda}(\Delta\theta, t)$:

$$r_{\omega\lambda}(\Delta\theta,t) = \frac{1}{2\pi j}\int_{\sigma-j\infty}^{\sigma+j\infty} e^{st}\cdot\left[R'(s)\cdot\frac{k}{s+k}\right]ds \qquad (D.5)$$

where $\sigma>0$.

The integrand of (D. 5) has the following singularities to the left of $s=\sigma$:

i) Simple poles at $s=j\omega n$, n odd.

ii) Simple poles at $s=j\omega n-a$, and at $s=-k$.

iii) Singularities due to $V(s-j\omega n)$.

iv) Simple poles at $s=j\omega m$, m even.

The residue at $s=j\omega n$ disappears on evaluation of the full expression, and the residues at (ii) and (iii) vanish in the limit as $t\to\infty$ (see before). Evaluating the residues as $s=j\omega m$, we obtain the following:

$$r_{\omega\lambda}(\Delta\theta,t) = \sum_{\substack{n\\ \text{odd}\\ -\infty}}^{+\infty}\sum_{n'}^{+\infty}\frac{4}{\pi^2}\cdot\frac{e^{jn2\pi\Delta\theta/\lambda}}{nn'}\left[\frac{1}{a+jn\omega}-\frac{1}{a+jn'\omega}\right] \cdot e^{j\omega(n+n')t}\cdot\frac{k}{k+j(n+n')\omega}\cdot W(n\omega)\,W(n'\omega) \qquad (D.7)$$

where $V(s)$ has been replaced by $W(\omega)$ (see Sec. 5.1), $\omega\Delta t$ has been replaced by $2\pi\Delta\theta/\lambda$ (q. v. Sec. 4.2), and $n'=m-n$.

This is the steady-state square-wave response of the modified H-unit.

References

Ditchburn, R. W., Ginsborg, B. L.: Involuntary eye-movements during fixation. J. Physiol. (Lond.) **119**, 1–17 (1953).

Dzn, H. de Lange: Relation between critical flicker frequency and a of low frequency characteristics of the eye. J. opt. Soc. Amer. **44**, 380–389 (1954).

Foster, D. H.: The perception of moving spatially-periodic intensity distributions. Optica Acta **15**, 625–626 (1968).

— The response of the human visual system to moving spatially-periodoc patterns. Vision Res. **9**, 577–590 (1969).

— Some experiments on the detection of motion by the human visual system and their theoretical interpretation. Ph. D. Thesis, University of London 1970a.

— The response of the human visual system to moving spatially-periodic patterns: Further analysis. Vision Res. in press (1970b).

Gilbert, D. S., Fender, D. H.: Contrast thresholds measured with stabilized and non-stabilized sine-wave gratings. Optica Acta **16**, 191–204 (1969).

Licklider, J. C. R.: A duplex theory of pitch perception. Experientia (Basel) **7**, 128–134 (1951).

Reichardt, W., Varju, D.: Übertragungseigenschaften im Auswertesystem für das Bewegungssehen. Z. Naturforsch. **146**, 674–689 (1959).

Spekreijse, H., Oosting, H.: Linearizing: A method for analysing and synthesizing nonlinear systems. Kybernetik **7**, 22–31 (1970).

Thorson, J.: Small signal analysis of a visual reflex in the Locust: II. Frequency dependence. Kybernetik **3**, 53–66 (1966).

Veringa, F.: On some properties of non-threshold flicker. J. opt. Soc. Amer. **43**, 500–502 (1958).

Dr. David H. Foster
Imperial College of Science
and Technology, Applied Optics
Section, Department of Physics
Prince Consort Road
London SW 7, England

Verantwortlich für den Textteil: Prof. Dr. W. Reichardt, D-7400 Tübingen, Max-Planck-Institut für biologische Kybernetik, Spemannstr. 38. — Verantwortlich für den Anzeigenteil: Edgar Seidler, D-1000 Berlin 15, Kurfürstendamm 237, Fernsprecher: (0311) 8833755, Telex: 01-82811. — Springer-Verlag, Berlin · Heidelberg · New York. — Druck der Universitätsdruckerei H. Stürtz AG, Würzburg. — Printed in Germany